

Study on absorbing properties of local resonance metamaterials and its application to noise reduction in ventilation

Randy Amuaku, Huabing WEN*, Zhiyuan Li, Djeuga Yamga, Yifeng Wu
School of Energy and Power, Jiangsu University of Science and Technology, Zhenjiang
212003, China

Abstract

Control of noise at low frequency is a huge challenge in engineering. The emergence of acoustic metamaterials generated a strong restitution of attention in noise control and reduction. Geometric and symmetric parameter constraints of local resonance frameworks serve as a foundation for improving acoustic metamaterial designs that achieve good results in low frequency. Phononic crystal bandgap characteristics is used to determine the direction and propagation of sound waves in low frequency mode. Characteristic analysis of bandgaps at low frequency and verification of rigid periodic split cylinder with a soft-core material scatterer inclusion was determined numerically and experimentally to show its acoustic characteristics in controlling low frequency noise. Numerical and experimental analysis of the PCs structure showed good noise absorption coefficient and insulation of noise in low frequency mode.

Keywords: Phononic crystal (PCs), Absorption Coefficient, Bandgap characteristics, Low frequency noise, Sound Insulation, Noise reduction, Acoustic metamaterials(AMMs).

1. Introduction

Sound and vibration of structures that are periodic have extensively been studied for decades because of their numerous applications in various engineering fields. Many types of structures that are periodic have been studied (Mead, 1996) such as stiffened plates/shells, tubes, lattice structures, etc. In recent years, propagation of waves in man-made structures that are periodic known as phononic crystals (PCs) (Sigalas & Economou, 1992) and acoustic metamaterials (AMMs) structures consisting of an array of elastic scatters inserted in a host membrane, have received renewed attention (Liu *et al.*, 2000). This paper is focused on merging the idea of PCs and AMMs in designing an acoustic engineering structure for the purpose of controlling noise at low frequency in ventilation units. The acoustic vibrations that attenuates in PCs have significant effects in its wave transmission irrespective of the direction of propagation in bandgap frequency ranges. The attenuation of acoustic locally resonating elements and their elastic waves have been studied extensively by various researchers over the past decade. Zhao *et al.*, experimentally verified the possibility of obtaining acoustic absorption at low-frequency using a local resonant sonic metamaterial (Zhao, Wen, Yu, & Wen, 2010). Guild *et al.*, researched on a sonic crystal acoustic metamaterial by designing an absorber based on the principle of an improved matching impedance and enhanced absorption (Zhang *et al.*, 2013). Recent research in acoustic metamaterial structures to attenuate sound includes the works of Christensen *et al.*, who used porous lamella materials exhibiting different parameter values and showed how random variation of material parameters can lead to an increased absorption of sound (Wen *et al.*, 2011). Starkey *et al.*, experimentally investigated a metamaterial structure to attenuate airborne sound at low frequency, which composed of a plate perforated with a deep subwavelength and a narrow channel for air flow separate from a rigid boundary (Starkey, Smith, Hibbins, Sambles, & Rance, 2017). Li, Y *et al.*, and Delany *et al.* researched on light weight structures, results showed broadband low-frequency absorption performance is possible by keeping the mass of the absorbing structure constant (Delany & Bazley, 1970; Li *et al.*, 2011). Mei, J. *et al.* researched on a double layer platelet arrays of aluminum reflector (Mei *et al.*, 2012) and achieved a perfect absorption at 164Hz with aluminum plate of thickness 58mm. Recently, local resonances have showed their potential for generating strong sound barriers and transparency (Liu *et al.*, 2000), and when viscoelastic or porous materials are combined, astonishing sound absorption effects is achieved (Wang, Casadei, Shan, Weaver, & Bertoldi,

2014).(Tang *et al.*, 2017), researched on hybrid acoustic metamaterial as a super absorber for broadband low frequency noise, results show that the absorber of thickness 60mm can achieve perfect absorption at 580Hz with high absorption bandwidth. Most recently, local resonance effects have been applied on ventilated metamaterials with promising results as in the works of Xiaoxiao Wu *et al.*, who researched on a high-efficiency ventilated metamaterial absorber at low frequency with numerical and experimental results showing high-efficiency absorption over 90%, the results also show that ventilated structures can obtain absorption by varying structural parameters(Wu *et al.*, 2018). In this paper, acoustic metamaterial specifically phononic crystals under Bragg scattering and local resonance mechanism principles is used to develop a novel sound absorptive structure for noise reduction at low frequency with an application in reducing noise between an air generating fan in a forced ventilation system and a ventilation duct distribution system in ship, marine vessels.

1.1. Low Frequency Bandgap

In this paper, we consider a cell with multiple split cylinders of different diameters within a square lattice. The cell structure is composed of aluminum, glass wool, epoxy and a polyurethane foam scatterer. The radius between the multiple split cylinders is given as r and a lattice constant a , $a = 24mm$, $r = 11.8mm \square 3.6mm$ with thickness of $0.6mm$ as shown in Fig.1,

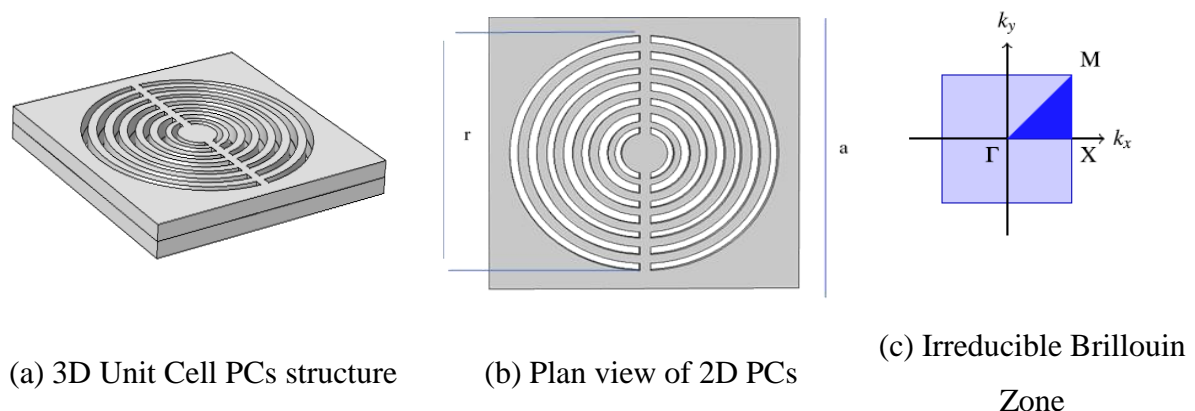


Fig. 1 Unit Cell Structure

Table. 1 Material Parameters

Material	Density
Aluminum	2700kg / m ³
Epoxy	1180kg / m ³
Glass wool	200kg / m ³
Polyurethane foam	1200kg / m ³

To investigate the bandgap characteristic and the resonant effects on the PCs structure, the bandgap characteristics were calculated for the infinite system by using finite element method (FEM). From Fig. 1 the unit cell is made up of two functional domains, blank regions show air domains while dark grey regions show solid domains. Applying acoustic sound pressure equation to the PCs model to calculate the band structure characteristics,

$$\nabla \left(\frac{1}{\rho} \nabla p \right) + \frac{\omega^2}{\rho c^2} p = 0 \quad (1.0)$$

where p is the sound pressure, ω is the angular frequency, C is the velocity of sound in air, and ρ (rho) represent the density of air. Due to the large acoustic impedance difference between aluminum and air in the solid membrane domain, the propagating sound waves in air is reflected by the aluminum plate. A Bloch-Floquet periodicity condition is applied on the PCs, as shown in equation,

$$p(r) = P(r + a)e^{-i(K.a)} \quad (2.0)$$

Where, r and a represent the vector position of the boundary node and the base vector of the crystal lattice respectively. The Bloch vector wave k is applied to define the phase relation of the planewave on the boundaries of the PCs. The sweep parameter k is a wave vector, which describes the differences in phase and defines boundary conditions between adjacent cell structures. With a given value of k defined, a group of eigenvectors and eigenvalues is obtained by solving the wave spectral problem. The k sweep parameter is varied in the first irreducible Brillouin zone to solve the spectra problem. The eigenvectors represent the sound pressure fields of eigenmodes. To study the model structure and resonant modes at frequencies where wave movement is prohibited, the bandgap characteristics is

calculated for the periodic unit cell using finite element method (FEM) in Comsol Multiphysics.

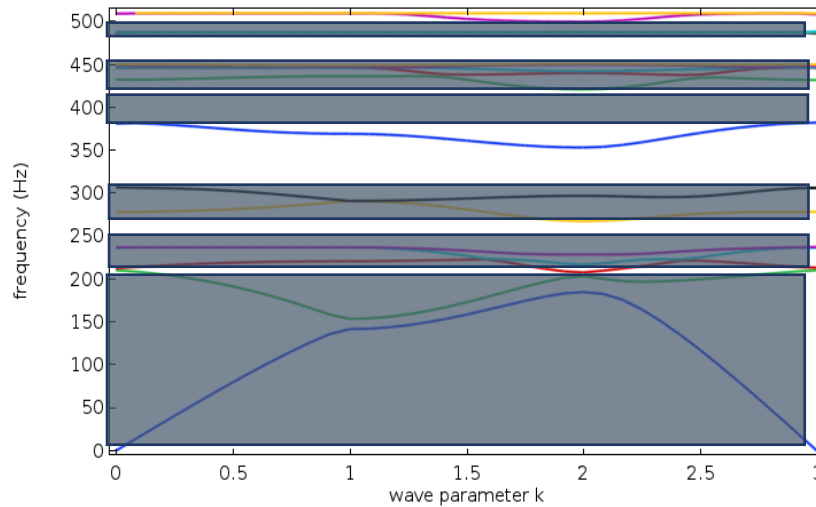


Fig.2 2D Bandgap structure of PCs $a_1 = a_2 = 24mm$ $r_1 = r_{14} = 11.8mm, 3.6mm$

The bandgap structure shows a wide gap between 0~200Hz in low frequency range. However, bandwidth of the subsequent bandgaps is relatively small comparing to the bandgap width of the wide gap between 0~200Hz. The bandwidth is reduced due to differences in thickness of the split cylinder inclusions.

1.2. Absorption Coefficient Model

The absorption coefficient of the model is predicted in comsol Multiphysics software, free and continuity boundaries is set between the different domains (solid/air). Plane wave radiation is applied at the top boundary, with an incident pressure field $p_{inc} = 1p_a$. However, the incident background pressure on the model surface is given as,

$$P_{inc} = e^{-i(K.x)} \tag{3}$$

Where, k is the wave number and x is the distance from the air-porous interface with the acoustic-poroelastic coupling condition applied horizontally. Johnson-Allard equivalent fluid model is applied on the PCs, according to the model the equation for effective bulk modulus and density of the rigid framed porous material comprise of five non-acoustical parameters given as tortuosity, flow resistivity, porosity thermal characteristics length and viscous

characteristics length respectively. Equation of effective density of the porous material surface is given by,

$$\rho(\omega) = \rho_o \alpha_\infty \left(1 + \frac{\sigma \phi}{i \alpha_\infty \rho_o \omega} G_j(\omega) \right) \quad (4)$$

where,

$$G_j(\omega) = \left(1 + \frac{4i \alpha_\infty^2 \eta \rho_o \omega}{\sigma^2 \Lambda^2 \phi^2} \right)^{\frac{1}{2}} \quad (5)$$

The bulk modulus equation is given as (6),

$$k(\omega) = \frac{\gamma p_o}{\left[\gamma - (\gamma - 1) \left| 1 + \frac{8\eta}{i \Lambda^2 \rho_o p r(\omega)} G_j'(p r \omega) \right|^{-1} \right]} \quad (6)$$

Where,

$$G_j'(\omega) = \left(1 + \frac{i \rho_o \Lambda^2 p r \omega}{16\eta} \right)^{\frac{1}{2}} \quad (7)$$

Viscous characteristic length and thermal characteristics length defined in equation (8), as presented by Champoux and Allard describes the thermic exchanges between the material frame and the pore saturating fluid considering the effective density of high frequency viscous and inertial effects,

$$\Lambda = \frac{1}{c} \left(\frac{8 \alpha_\infty \eta}{\sigma \phi} \right)^{\frac{1}{2}}, \quad (8)$$

$$\Lambda' = \frac{1}{c'} \left(\frac{8 \alpha_\infty \eta}{\sigma \phi} \right)^{\frac{1}{2}}$$

Where ρ_o is the density of air, α_∞ is the tortuosity, σ is the flow resistivity, ϕ is the porosity of porous material, ω is the angular frequency, f is the frequency of sound, i is an imaginary number, Λ is the viscous characteristics length, Λ' is the thermal characteristics length, η is the viscosity of the air, γ is the specific heat ratio of the air and p_o is the atmospheric pressure. The porous material characteristics impedance Z_s is derived from the

effective density $\rho(\omega)$ and bulk modulus $k(\omega)$ using Eq. (9), $G_j(\omega)$ and $G_j'(\omega)$ are the correction functions introduced respectively by Johnson et al. and by Champoux and Allard(Allard, Dazel, Gautier, Groby, & Lauriks, 2011), ℓ is a parameter that depends on the split ring diameter and thickness. Characteristic Impedance of the surface is given as Z_c ,

$$Z_c(\omega) = [\rho(\omega)k(\omega)]^{\frac{1}{2}} \quad (9)$$

Applying Specific Heat ratio of air γ

$$\gamma = \frac{j\omega}{c_o} \sqrt{1 + \frac{\sigma}{j\omega\rho_o}} \quad (10)$$

For a layer of porous material with thickness d' backed by a reflecting hard surface, the reflection coefficient can be evaluated from the porous material surface characteristic impedance Z_s as,

$$Z_s(\omega) = \frac{Z_c}{\phi} \coth(m_c d) = -i \frac{Z_c}{\phi} \cot(k_c d) \quad (11)$$

where, m_c denotes the complex wave propagation constant,

$$m_c(\omega) = i\omega \left[\frac{\rho(\omega)}{k(\omega)} \right]^{\frac{1}{2}} \quad (12)$$

From equation (9), applying complex wave number k_c as,

$$k_c(\omega) = \omega \left[\frac{\rho(\omega)}{k(\omega)} \right]^{\frac{1}{2}} \quad (13)$$

From equation (9), $c_o = 343m/s$ and $\rho_o = 1.25kg/m^3$, the reflecting surface coefficient of the model is giving by,

$$R = Z_s = -i \frac{[\rho(\omega)k(\omega)]^{\frac{1}{2}}}{\phi} \cot(\omega \left[\frac{\rho(\omega)}{k(\omega)} \right]^{\frac{1}{2}} * d) = \left[\frac{Z_s - 1}{Z_s + 1} \right]^2 \quad (14)$$

by substituting equation(9)&(13) into equation (11), reflection coefficient of the model surface of a semi-infinite layer of an absorptive material can be obtained as,

$$\text{Absorption Coefficient } \alpha = 1 - |R|^2 \quad (15)$$

2. Experimental Analysis

The experimental set-up is presented in Fig. 3. It comprises of a cylindrical tube of internal diameter 60mm. The cylindrical tube serves as a resonator. The experiment was conducted within a frequency range of 20~2000Hz and 25~2500Hz to study the characteristic behavior of the phononic crystal structure in low frequency range. The source of sound is situated at one end of the cylindrical tube to generate plane wave which propagates towards the phononic crystal structure placed at the other end of the cylindrical tube. The experiment was conducted such that the measurement configuration, that is the sound emitted by the source is a swept sine. Two microphones were used in the experiment, one microphone is inserted into the cylindrical tube by clamping it perpendicularly towards the source of sound source to appreciate all the sound pressure emanating from the source of sound whiles the other microphone is placed behind the PCs structure. Frequency response functions between the inserted microphone and the one placed outside at a distance behind the PCs structure is recorded by a data acquisition system. In the experiment, to reduce feedback errors in the cylindrical tube the reference signal which is an input controller conveys the signals into the cylindrical tube through a loudspeaker. The experiment is conducted on the PCs structure by clamping it to the flange of the cylindrical tube with nuts and bolts for the frequency analysis and measurement.

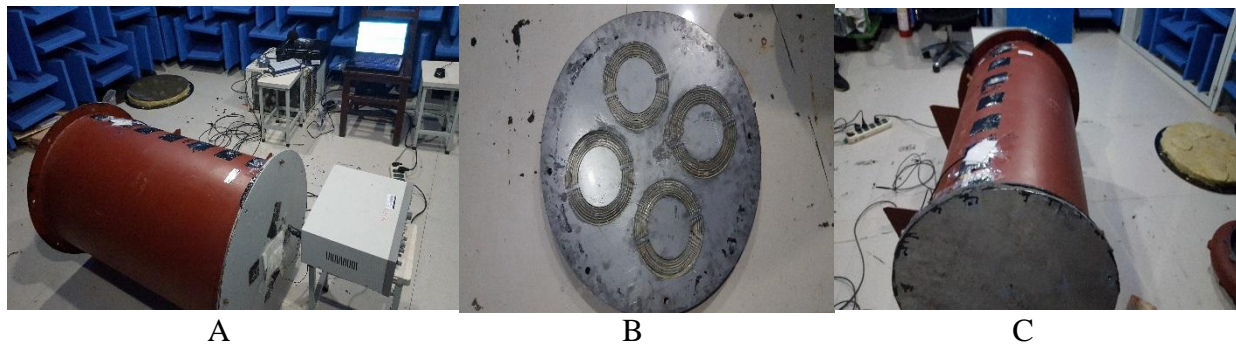


Fig 3 Experimental setup

2.1 Results and Discussion

Numerical prediction of the absorption coefficient of the porous surface of the model in comsol multiphysics showed a noise absorption value of 0.89. The experiment conducted on the PCs structure to verify its sound insulation ability showed good results in low and high frequency range. The results of the PCs structure show an ascending noise insulation curve with a gradual increase from low to high insulation ranges. The PCs structure at frequency of 167.6Hz had a noise reduction of 44.5dB and at a frequency of 630Hz had a noisereduction of 53.7dB in the experiment conducted with a cylindrical tube serving as an impedance tube. The base membrane rigid damping and density had effects on the PCs structure's sound insulation. The numerical noise prediction and the experimental results are in agreement. The noise absorption and insulation values from the prediction and experiment is converted into decibels and presented in Fig.4.

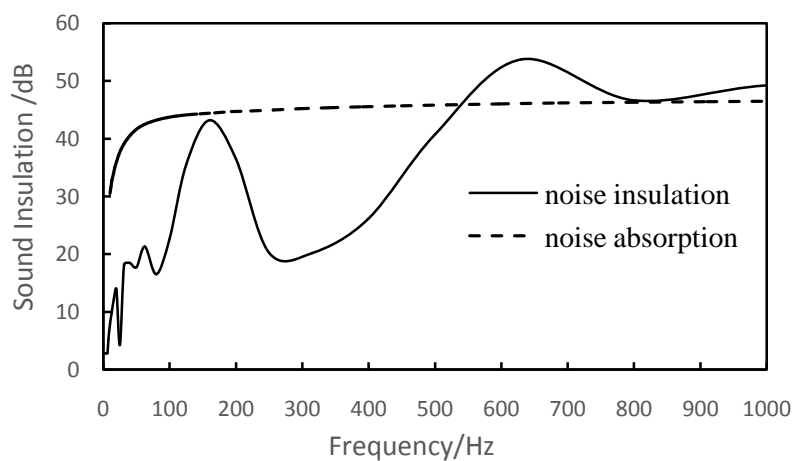


Fig.4 Noise Absorption and Insulation

In predicting the noise reduction of the PCs structure within a duct system, it is placed between an air generating fan system and a ventilation duct system in a ship to know the amount of noise in decibels the PCs structure can obstruct before the air enters the ventilation duct system. Applying the principle of transmission loss;

$$TL = -20 \log_{10} \left| \frac{P_i}{P_o} \right| \quad (16)$$

where, P_i is the acoustic pressure of the incident wave in the inlet, P_o is the acoustic pressure of the reflected wave in the outlet. A low transmission loss of -142 dB was obtained at a frequency of 290Hz.

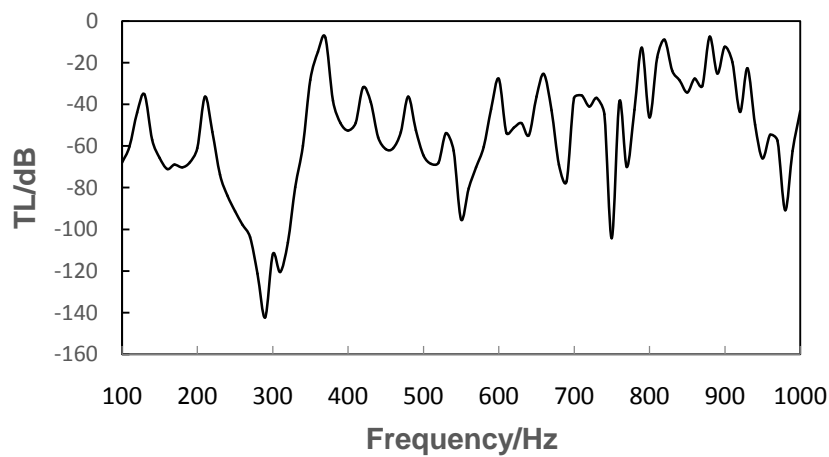


Fig. 5 Noise Transmission Loss

3. Conclusion

In this paper, the sound absorbing properties of local resonance acoustic metamaterial (PCs) with a periodic split cylinder inclusion has being studied. Johnson-Allard equivalent fluid model was used to predict the absorption coefficient characteristics of the porous model surface. The experiment results demonstrated that with a rigid membrane support a porous material surface can obtain good noise reduction characteristics in low frequency ranges. In summary the following observations have been made,

- the acoustic insulation of a porous material surface can be improved when the support membrane is rigid, causing the porous membrane to behave as a damper when sound pressure incident on its surface.
- the PCs structure has good sound absorption at frequencies 167.6Hz and 630Hz by obtaining noise insulation of 44.5dB and 53.7dB respectively.
- the PCs structure at a frequency of 290Hz has noise transmission loss of -142 dB
- the structure based on numerical and experimental results has useful application in noise reduction and ventilation.

Reference

- Allard, J.-F., Dazel, O., Gautier, G., Groby, J.-P., & Lauriks, W. (2011). Prediction of sound reflection by corrugated porous surfaces. *The Journal of the Acoustical Society of America*, 129(4), 1696-1706.
- Delany, M., & Bazley, E. (1970). Acoustical properties of fibrous absorbent materials. *Applied acoustics*, 3(2), 105-116.
- Li, Y., Wang, X., Wang, X., Ren, Y., Han, F., & Wen, C. (2011). Sound absorption characteristics of aluminum foam with spherical cells. *Journal of Applied Physics*, 110(11), 113525.
- Liu, Z., Zhang, X., Mao, Y., Zhu, Y., Yang, Z., Chan, C. T., & Sheng, P. (2000). Locally resonant sonic materials. *Science*, 289(5485), 1734-1736.
- Mead, D. (1996). Wave propagation in continuous periodic structures: research contributions from Southampton, 1964–1995. *Journal of sound and vibration*, 190(3), 495-524.
- Mei, J., Ma, G., Yang, M., Yang, Z., Wen, W., & Sheng, P. (2012). Dark acoustic metamaterials as super absorbers for low-frequency sound. *Nature communications*, 3, 756.

- Sigalas, M. M., & Economou, E. N. (1992). Elastic and acoustic wave band structure. *Journal of sound and vibration*, 158(2), 377-382.
- Starkey, T., Smith, J., Hibbins, A., Sambles, J., & Rance, H. (2017). Thin structured rigid body for acoustic absorption. *Applied Physics Letters*, 110(4), 041902.
- Tang, Y., Ren, S., Meng, H., Xin, F., Huang, L., Chen, T., . . . Lu, T. J. (2017). Hybrid acoustic metamaterial as super absorber for broadband low-frequency sound. *Scientific Reports*, 7, 43340.
- Wang, P., Casadei, F., Shan, S., Weaver, J. C., & Bertoldi, K. (2014). Harnessing buckling to design tunable locally resonant acoustic metamaterials. *Physical review letters*, 113(1), 014301.
- Wen, J., Zhao, H., Lv, L., Yuan, B., Wang, G., & Wen, X. (2011). Effects of locally resonant modes on underwater sound absorption in viscoelastic materials. *The Journal of the Acoustical Society of America*, 130(3), 1201-1208.
- Wu, X., Au-Yeung, K. Y., Li, X., Roberts, R. C., Tian, J., Hu, C., . . . Wen, W. (2018). High-efficiency ventilated metamaterial absorber at low frequency. *Applied Physics Letters*, 112(10), 103505.
- Zhang, Y., Wen, J., Zhao, H., Yu, D., Cai, L., & Wen, X. (2013). Sound insulation property of membrane-type acoustic metamaterials carrying different masses at adjacent cells. *Journal of Applied Physics*, 114(6), 063515.
- Zhao, H., Wen, J., Yu, D., & Wen, X. (2010). Low-frequency acoustic absorption of localized resonances: Experiment and theory. *Journal of Applied Physics*, 107(2), 023519.